Neutron Diffraction Study on the Mechanism of the Topotactic Reduction of 2H–TaS₂ Electrodes

C. RIEKEL

Institut Max von Laue–Paul Langevin, 38042 Grenoble, France

AND H. G. REZNIK AND R. SCHÖLLHORN

Anorganisch-chemisches Institut der Universität, 4400 Münster, West Germany

The dynamic investigation by neutron diffraction of the topotactic reduction of 2H–TaS₂ electrodes in K^+/D_2O electrolyte to the ionic layered hydrate $K_{0.5}^+(D_2O)_{0.5}[TaS_2]^{0.5-}$ is shown to proceed via third-stage $K_x^+(D_2O)_y[TaS_2]_3^{x-}$, second-stage $K_x^+(D_2O)_y [TaS_2]_2^{x-}$, and first-stage $K_x^+(D_2O)_y[TaS_2]^{x-}$ intermediates. A comparative study by X-ray diffraction on the cathodic intercalation of 2H–TaS₂ and 2H–NbS₂ electrodes with hydrated main group and transition metal ions reveals analogous behavior; the formation of higher-stage intermediates is supposedly correlated with stable electronic layer states. Influence of kinetic factors is observed for larger guest cations such as transition metal complexes and organic ions. CdI₂-type host lattices with an octahedral environment of intralayer cations shown different reaction pathways, although the occurrence of intermediate states (at least in the nucleation phase) can be demonstrated. It is concluded that the presence of ordered intermediate states is a general phenomenon in topotactic electrode processes of layered dichalcogenides.

Introduction

The formation of intercalation compounds of layered dichalcogenides MX_2 (M = transition metal, X = chalcogen) by cathodic or chemical reduction in aqueous and nonaqueous electrolytes has originally been reported by several authors (*1–4*). We were able to show that this reaction proceeds reversibly and is to be described as a topotactic redox reaction leading to intercalation phases with ionic structures, the electrons being taken up by the conduction band of the metallic layers (*1, 4, 5*). In the case of strongly polar electrolyte solvents, e.g., H_2O, the cations A^{z+} enter the lattice as solvated ions $A^{z+}(H_2O)_y$ (Eq. (1)) and the resulting phases show polyelectrolyte behavior, i.e.,

$$\frac{x}{z} A^{z+} + y\,H_2O + MX_2 + x\,e^-$$
$$\rightleftharpoons (A^{z+})_{x/z}(H_2O)_y[MX_2]^{x-}, \quad (1)$$
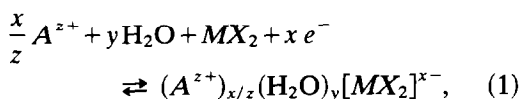
ion and solvate exchange (*5*). So far in most cases only the final reaction products obtained on quantitative reduction have been characterized with respect to composition and basic structure and no detailed experimental information is available as concerns the reaction mechanism, although the observation of discrete potential steps in potential/time curves was attributed to the occurrence of second-stage-type intermediates (*1*).

253

Kinetic studies by neutron diffraction were shown by us recently to represent a novel efficient technique for the structural characterization of transient processes and intermediates in the course of intercalation reactions (6, 7) owing to (i) the high scattering contribution of light atoms as compared to that of X-ray diffraction, (ii) the possibility to avoid sample transfer during the reaction, which may lead to uncontrollable changes in the case of susceptible or unstable phases, and (iii) the fact that transmission spectra are obtained and the integral structural changes of the sample volume are measured as compared to X-ray diffraction (8), where only regions close to the sample surface contribute to the diffraction pattern and complications may thus arise.

The application of neutron diffraction in a recent study by us to the cathodic reduction of $2H-TaS_2$ in D_2O/D_2SO_4 under formation of D_xTaS_2 demonstrated conclusively the possibility of a direct transient examination of topotactic electrode processes by this method (7). In the present communication we report our results of a neutron diffraction study on the mechanism of formation of $K_x^+(H_2O)_y[TaS_2]^{x-}$ by galvanostatic cathodic reduction of $2H-TaS_2$ electrodes in aqueous electrolyte along with a comparison to reactions of related layered phases based on X-ray data.

Experimental

All starting materials used for chemical preparations were reagent grade. $2H-TaS_2$ was obtained by heating the elements to 900°C/10 days in evacuated quartz ampoules and subsequent annealing at 400–500°C/10 days. Cathodic reduction of pressed powder and single-crystal $2H-TaS_2$ electrodes was performed at 23°C in aqueous electrolytes containing 0.1–1 M solutions of the cationic species to be intercalated; further details are described in earlier publications (1, 7). Composition was determined by wet analysis and atomic absorption spectrometry. X-ray powder and single-crystal techniques served for structural characterization of the samples.

Neutron diffraction work was performed on the D1B diffractometer (ILL Grenoble) at a wavelength of 2.4 Å (6, 7). Two different cross sections of the electrochemical cell used for the neutron diffraction study and the orientation of the cell relative to the neutron beam are shown schematically in Fig. 1. A cylindrical quartz vessel served as the container for the cell constituents; it was filled with 1 M K_2SO_4 in D_2O as the electrolyte. Two platinum counter electrodes were positioned symmetrically to the central working electrode; cathode and anode compartments were separated by quartz
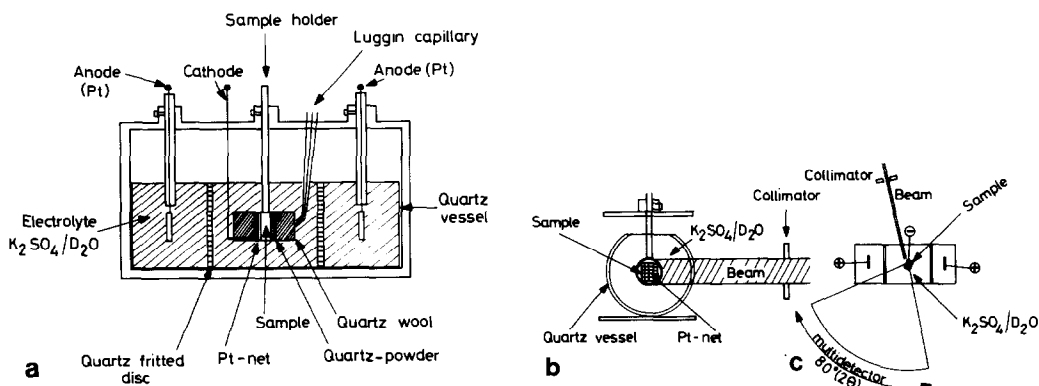
FIG. 1. Scheme of electrochemical cell for neutron diffraction study; (a, b) cross section; (c) orientation of cell and sample on the D1B diffractometer.

fritted disks. The polycrystalline 2H–TaS$_2$ sample (4 g) was shaped into a cylindrical pellet of the approximate dimensions 13 × 5 mm (diameter × height) by a pressure of 6 tons cm^{-2}. The working electrode was placed in a short separate quartz tube and fixed elastically by quartz powder and quartz wool in order to account for the volume increase and resulting mechanical stress during intercalation. A platinum net served for electrical connection with the TaS$_2$ electrode. The reference electrode (Ag/AgCl) was connected via a quartz Luggin capillary with the working electrode. The reduction process (reaction temperature, 23°C) was controlled by a commercial high-precision potentiostat at constant current; an X/t recorder was used for continuous recording of the working electrode potential as measured vs a Ag/AgCl electrode.

Recording time for spectra was 15 min with an interval of 1–2 sec between consecutive spectra. The time resolution obtained thus proved to be sufficient to interpret the structural variations encountered during the reaction. Data analysis has been described earlier (6, 7). Synchronously with the recording of the spectra the degree of reduction at constant current (5 mA) was controlled by the galvanostatic equipment. K$^+$ content determined analytically after a transfer of 0.07, 0.11, 0.21, and 0.5 e^- was 0.06, 0.1, 0.19 and 0.44 K$^+$/Ta, respectively. The values are somewhat lower than those calculated from electrochemical data which is due to the loss of K$^+$ by protolysis on removal of the electrolyte phase by washing with N$_2$-saturated water.

Intercalation of alkaline earth ions, transition metal ions, complex ions, and organic cations was performed as described above; the binary chalcogenides 2H–NbS$_2$, TiS$_2$, and 1T–TaS$_2$ were prepared by vapor-phase transport from the elements at 800–900°C. X-Ray Guinier powder data (CuKα radiation) served for the evaluation of structural data of the products. For the metal complex

intercalation compounds reported the following compositions were obtained from analytical data after washing of the samples with water: Co/Ta = 0.24 for (C$_5$H$_5$)$_2$Co$^+$, Cr/Ta = 0.14 for (C$_6$H$_6$)$_2$Cr$^+$, Fe/Ta = 0.11 for [Fe(phenanthroline)$_3$]$^{2+}$, Cu/Ta = 0.13 for [Cu(en)$_2$]$^{2+}$, Pt/Ta = 0.15 for [Pt(NH$_3$)$_4$]$^{2+}$.

Results and Discussion

The layered dichalcogenides of transition elements MX_2 are electronically conducting solids with hexagonal lattice symmetry which are built up by two-dimensional sandwich-type X–M–X units held together in the crystal lattice by van der Waals forces. On quantitative cathodic reduction of single-crystal or polycrystalline MX_2 electrodes in aqueous alkali salt solutions two different types of hydrates $A_x^+(H_2O)_y[MX_2]^{x-}$ ($x_{max} = 0.5$) are observed with monolayers and bilayers, respectively, of water between the dichalcogenide sheets depending on the cation hydration energy (5). The interlayer distance d between neighboring MX_2 units amounts to ca. 9 Å in the monolayer case, i.e., the sum of the MX_2 layer dimension perpendicular to the layer planes (ca. 6 Å) and the diameter of the H$_2$O molecules (ca. 3 Å). In the case of bilayer hydrates d is found to be 6 Å + 2 × 3 Å = 12 Å.

For the present investigation on the course of the cathodic reduction of dichalcogenide electrodes in strongly polar solvents we decided to examine the formation of K$_{0.5}^+$(D$_2$O)$_{0.5}$[TaS$_2$]$^{0.5-}$ from 2H–TaS$_2$ and D$_2$O/K$^+$ electrolyte because of the fairly high stability of the reaction product and the small particle size of the starting material which reduces potential kinetic effects. D$_2$O was used instead of H$_2$O in order to suppress the incoherent scattering of hydrogen (6); X-ray diffraction and electrochemical studies revealed no difference in behavior between the two solvents.

The overall reaction scheme is given in Eq. (2); the interlayer distance of the solvated potassium phase amounts to 9.04 Å (monolayer hydrate).

$$0.5\,K^+ + 0.5\,e^- + 0.5\,D_2O + TaS_2 \rightarrow$$

$$K_{0.5}^+(D_2O)_{0.5}[TaS_2]^{0.5-} \quad (2)$$
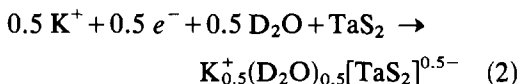
As a consequence of the high mobility at room temperature of the guest-phase constituents the structure of the product phase could be partially resolved only in a single-crystal X-ray study (9). ^1H NMR studies revealed, however, the strongly anisotropic mobility of water molecules in the hydrate phase (10).

The potential/charge transfer curve for the galvanostatic reduction of polycrystalline 2H–TaS$_2$ electrodes in D$_2$O/K$_2$SO$_4$ (n = Faraday/mole TaS$_2$) is shown in Fig. 2; the curve is identical to that obtained in H$_2$O electrolyte. On a phenomenological base the curve may be divided into different regions A–E according to the changes appearing in potential slope. After a transfer of 0.48–0.5 e^-/TaS$_2$ a plateau is reached (E) that corresponds to the potential of D$_3$O$^+$ ion discharge; throughout the reduction process of the solid the potential measured vs Ag/AgCl remains close to the equilibrium potential at the current density applied. The shape of the galvanostatic curve and the length of the different regions are not
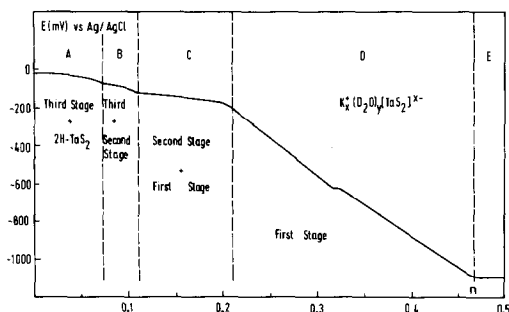
FIG. 2. Galvanostatic reduction of 2H–TaS$_2$ in D$_2$O/K$_2$SO$_4$. Potential (E vs Ag/AgCl) as a function of charge transfer n = Faraday/mole TaS$_2$; i = 5 mA.

affected by changes in K$^+$ concentration between 0.1 and 2 M, by the particle size of the starting material, and by the pressure applied in the preparation of pressed electrodes.

In Fig. 3a the integrated relative intensities I (6) of characteristic reflections observed at low 2Θ values are plotted versus charge transfer n. For $n > 0$ a rapid decrease in intensity of the (002) reflection of the host lattice 2H–TaS$_2$ is noted along with the appearance of the reflection of a new phase designated as P1 with $d \sim 5.1$ Å, whose intensity increases with the degree of reduction. After a transfer of 0.07 e^-/TaS$_2$ the intensity of the host lattice reflection has decreased to a small fraction of the original value; at $n \cong 0.11$ the intensity of the P1 line starts to decrease now between $n \cong 0.11$ and $n \cong 0.21$. Simultaneously the reflection of a novel phase P2 with $d = 4.57$ Å initially appears and increases in intensity in the range of $n = 0.11$ to $n = 0.21$. As for similar intercalation reactions we assign both P1 and P2 to (00l) reflections (6, 7); the maximum intensities are found at $n = 0.11\,e^-$/TaS$_2$ for P1 and $n = 0.22\,e^-$/TaS$_2$ for P2. After normalizing the intensities to 1.0 at these points it can be shown that no further phase is formed in section C, i.e., $I(P1) + I(P2) = 1$; C is therefore a two-phase region. In sections A and B we find $I(002/TaS_2) + I(P1) > 1$. The peak position of P1 is not constant as is to be expected for a single defined phase. The data analysis (Fig. 3b) suggests three ranges: (i) $d = 5.19$ Å for $0 < n < 0.07$, (ii) 5.19 Å $> d > 5.00$ Å for $0.07 < n < 0.12$, and (iii) $d = 5.00$ Å for $n > 0.12$ which correspond fairly well with the changes in potential slope in the potential/charge transfer curve (Fig. 2). A similar although less-well-defined change in peak position was observed earlier for TaS$_2$·(ND$_3$)$_{1-x}$ upon transformation of third-stage "bulk" nuclei into second-stage bulk nuclei (6). The origin of this effect is due to the fit of one Gaussian profile to a profile with two closely neighboring peaks. It was
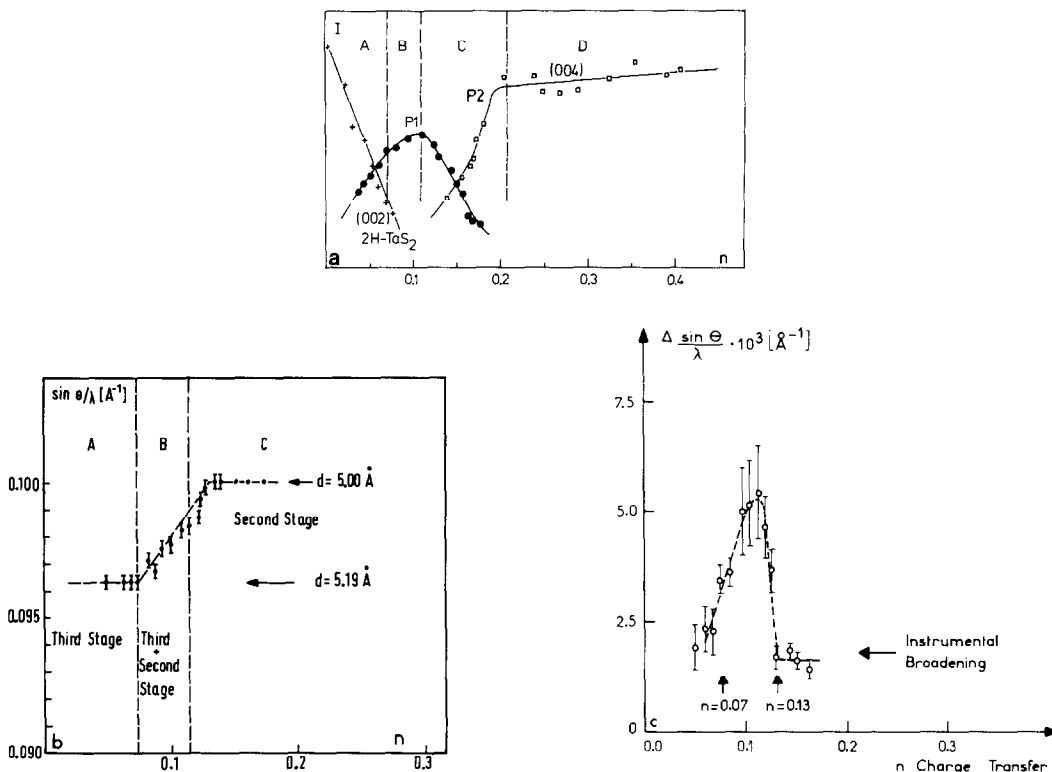
FIG. 3. Galvanostatic reduction of 2H-TaS₂. (a) Relative intensities I of characteristic neutron diffraction lines as a function of charge transfer n; (b) peak position of P1 reflection as a function of n; (c) FWHH of P1 reflection as a function of n.

not possible in the present case to separate the two peaks sufficiently well as both $2d$ and $3d$ stages (see below) exhibit broadened reflections probably due to statistical disorder in the layer sequence (11). The model proposed is, however, supported by the change in full width at half-height (FWHH) of the P1 reflection which corresponds to the instrumental broadening for ranges A and C but increases significantly for range B (Fig. 3c).

For further analysis of the diffraction data the following assumptions and statements, respectively, are considered: (i) a change in stacking sequence is induced in the course of the intercalation reaction leading to trigonal prismatic interlayer positions; this process has been observed so far for all intercalation reactions with 2H-TaS₂; (ii) interlayer posi-

tions not occupied by K^+ are filled up with D_2O molecules; since the K^+ amount in the pure phases must be proportional to the charge transferred at the phase border line, the D_2O amount can be evaluated—via the formula $(K^+)_x(D_2O)_y[TaS_2]_m^{x-}$ and the maximum number of D_2O/K^+ positions that can be occupied—by the correlation $x + y = 1$ for an idealized lattice; (iii) the layer dimension perpendicular to the layer plane is 6.05 Å and the lattice expansion for one K^+/D_2O layer in direction of the hexagonal c axis amounts to ca. 3 Å(5); (iv) the diffusion of D_2O and K^+ is too rapid at room temperature to be observed on the time scale of the present measurements; only accumulation and depletion of phases is detected.

The thickness of a D_2O monolayer is rather similar to that of a NH_3 layer. In

analogy to the TaS_2/NH_3 system we assign therefore the reflection with $d = 5.19$ Å to (008) of a third-stage phase ($d_{calc} = 5.25$ Å) and the reflection with $d = 5.0$ Å to (006) of a second-stage compound ($d_{calc} = 5.0$ Å). The hexagonal c axes resulting are $c = 42$ Å for the third-stage compound and $c = 30$ Å for the second-stage compound. From the neutron diffraction data and the characteristic changes in potential slope (Fig. 2) the stoichiometries of the third- and second-stage phases can be evaluated as

$$K_{0.07}^+(D_2O)_y[TaS_2]^{0.07-} =$$

$$K_{0.21}^+(D_2O)_{0.79}[TaS_2]_3^{0.21-}$$

and

$$K_{0.11}^+(D_2O)_y[TaS_2]^{0.11-} =$$

$$K_{0.22}^+(D_2O)_{0.78}[TaS_2]_2^{0.22-};$$

complete occupation of all trigonal prismatic interlayer positions by K^+ and D_2O, respectively, is thereby assumed (Fig. 4). Sections A and B of Fig. 2 represent thus two-phase regions $TaS_2/3d$ stage and $3d$ stage/$2d$ stage.

The presence of a second-stage compound at the intersection B/C (Fig. 2) is substantiated further by the results of ion exchange reactions of TaS_2 reduced to $n = 0.11$ according to Eq. (3). The exchange was found to proceed,

$$(K^+)_{0.22}(H_2O)_{0.78}[TaS_2]_2^{0.22-}$$

$$+ 0.22 \, Na^+ + yH_2O \rightleftharpoons$$

$$(Na^+)_{0.22}(H_2O)_{0.78+y}[TaS_2]_2^{0.22-}, \quad (3)$$

quantitatively and reversibly; as Na^+ induces the formation of water bilayers a change in the interlayer spacing from $d = c/2 = 15.3$ Å (K^+ phase) to $d' = c/2 = (2 \times 6$ Å$) + (2 \times 3$ Å$) = 18$ Å is to be expected. The interlayer spacing measured by X-ray diffraction for the Na^+ exchanged form was found to be 18.2 Å and corresponds well with similar values observed for second-stage bilayer hydrates obtained earlier (5).

FIG. 4. Scheme of structural transformations during galvanostatic reduction of $2H$–TaS_2.

In the two-phase range C the second-stage compound and P2 coexist. Pure P2 is present at the intersection C/D; its composition calculated via the corresponding charge transfer of $0.22 \, e^-/TaS_2$ is equivalent to $(K^+)_{0.22}(D_2O)_{0.78}[TaS_2]_2^{0.22-}$. If we assign the P2 reflection at 4.57 Å to (004) of a first-stage phase (all van der Waals gaps occupied; Fig. 4) with an interlayer spacing of 9 Å (6 Å for TaS_2 layer + 3 Å for D_2O/K^+ layer) a c axis value of 18 Å results, if K^+ and D_2O reside in trigonal prismatic positions. The (004) reflection showed only instrumental broadening with full width at half-height $0.5°/2\Theta$. The identification of P2 with a first-stage phase was again confirmed by ion exchange reaction of TaS_2 reduced in K^+/H_2O to $n = 0.22 \, e^-/TaS_2$ with Na^+/H_2O resulting in the formation of the corresponding sodium hydrate with water bilayers and an interlayer spacing of $d = c/2 = 11.9$ Å (6 Å$ + 2 \times 3$ Å$)$ (5).

It is surprising that the interlayer cation density is approximately identical for all three stages observed up to $n = 0.22$. The formation of higher stages could be due either to a particular stability of the "two-dimensional" interlayer electrolyte phase at this composition or due to an electronic instability of first-stage phases with single layers of negative charge densities lower than $0.2 \, e^-/TaS_2$. We shall come back to that point later. There remains still the problem of the mechanism of the transition third stage to second stage; similar transitions have been

observed in the case of graphite intercalation compounds and were explained in terms of the intergrowth of two or more stages (12). It is open to question whether a similar mechanism applies to the layered dichalcogenides.

Further reduction beyond $0.22\ e^-/\mathrm{TaS}_2$ proceeds at approximately constant interlayer spacing with the synchronous uptake of K^+ ions and electrons into the lattice under expulsion of a corresponding number of $\mathrm{H}_2\mathrm{O}$ molecules (Eq. (4)). The final product of the reduction is $\mathrm{K}^+_{0.45}(\mathrm{D}_2\mathrm{O})_{0.55}[\mathrm{TaS}_2]^{0.45-}$ with the hexagonal axes $a = 3.33$ Å, $c = 18.18$ Å as determined by X-ray diffraction.

$$(\mathrm{K}^+)_{0.22}(\mathrm{D}_2\mathrm{O})_{0.78}[\mathrm{TaS}_2]^{0.22-}$$

$$+ z\,\mathrm{K}^+ + z\,e^- \rightarrow$$

$$(\mathrm{K}^+)_{0.22+z}(D_2O)_{0.78-z}[\mathrm{TaS}_2]^{(0.22+z)-}$$
$$+ z\mathrm{D}_2\mathrm{O} \quad (4)$$
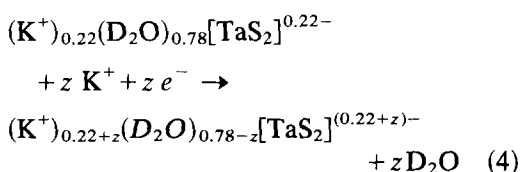
From the slope of the potential charge transfer curve it may be concluded qualitatively that D corresponds to a nonstoichiometric phase range. These conclusions are currently under investigation on the structural side by a long-wavelength neutron diffractometer for polycrystalline samples as well as by single-crystal studies. We found that TaS$_2$ electrodes in Na$^+$/D$_2$O give essentially results closely similar to those of the K$^+$ system with the appearance of first-, second-, and third-stage compounds; the degree of ordering of the intermediates in ranges A and B is, however, considerably higher in the Na$^+$ case and a higher number of general reflections is observed.

An extended investigation on the intercalation by cathodic reduction of hydrated cations differing in charge and dimension revealed that the occurrence of higher-stage intermediates in the starting range of the reaction is not restricted to alkali ion derivatives but seems to be a rather general phenomenon for 2H–NbS$_2$ and 2H–TaS$_2$ as the host lattice. In view of the relatively large number of systems the study had to be carried out by X-ray diffraction methods. Data for a series of hydrated alkaline earth, transition metal, and main group metal ion intercalation compounds are listed in Table I. Potential/charge transfer curves for these phases are all characterized by a step in potential after a transfer of $0.6-0.8\ e^-/\mathrm{TaS}_2$ and $0.1-0.13\ e^-/M\mathrm{S}_2$ similar to that in Fig. 2. X-Ray data show that in this reduction range two-phase regions with the presence of third- and second-stage compounds exist. As a consequence of the high charge/radius ratio of the cations all of the compounds listed are bilayer hydrates (5) with interlayer spacings of ca. 12 Å (6 Å + 2 × 3 Å) for the first-stage final product and of ca. 18 Å(2 × 6 Å + 2 × 3 Å) for the second-stage product (Table I). Diffraction line broadening is observed for all second-stage intermediates, whereas normal linewidths are found for the first-stage compounds. The maximum degree of reduction extends to $0.4-0.5\ e^-/M\mathrm{S}_2$.

The systematic occurrence of higher-stage phases for cations of different charge and radius leads us to the assumption that the formation of these intermediates is not due to the stability of interlayer hydrate structures with a particular composition but is governed by electronic aspects (cf above).

Kinetic reasons, seem, however, to become of importance, if larger cations with low hydration energy are considered. The intercalation of transition metal complex cations proceeds readily from aqueous and nonaqueous electrolytes and the interlayer spacing values observed agree reasonably well with the cation dimensions (Table II). Potential/charge transfer curves show, however, no defined steps in most cases. X-Ray photographs taken at low charge transfer values show lines of the first-stage product in addition to broad diffraction lines at lower 2Θ values indicating the presence of higher stages. Even at low current densities the potentials measured are considerably lower than the corresponding equilibrium

TABLE I

LAYERED HYDRATED CHALCOGENIDES
OBTAINED BY CATHODIC REDUCTION
OF 2H–TaS$_2$ AND 2H–NbS$_2$ IN
AQUEOUS ELECTROLYTES[a]

A^{z+}	M	d (Å)	d' (Å)	n
Mg^{2+}	Nb	11.74	17.8	0.13
	Ta	11.98	17.9	0.11
Ca^{2+}	Nb	11.77	18.2	0.12
	Ta	11.88	18.1	0.12
Sr^{2+}	Nb	11.84	18.2	0.13
	Ta	11.95	17.9	0.11
Ba^{2+}	Nb	11.90	18.3	0.12
	Ta	11.99	18.4	0.13
Cr^{3+}	Ta	11.92	17.7	0.13
Mn^{2+}	Nb	11.81	17.9	0.13
	Ta	11.98	18.2	0.13
Fe^{2+}	Nb	11.72	18.3	0.12
Co^{2+}	Nb	11.71	17.7	0.13
	Ta	11.68	17.8	0.14
Ni^{2+}	Nb	11.51	17.9	0.13
Zn^{2+}	Ta	11.27	18.1	0.13
Ce^{3+}	Ta	12.91	17.9	0.13
La^{3+}	Ta	12.89	18.0	0.12

[a] A = interlayer cation; d = interlayer spacing of first-stage phase $A_{x/z}^{z+}$ $(H_2O)_y[MS_2]^{x-}$ (final reaction product); d' = interlayer spacing of second-stage phase; n = charge transfer value (Faraday/mole MS_2) at the upper limit of the two-phase region $3d$ stage/$2d$ stage; M = intralayer transition metal ion.

values. An exception is $[Pt(NH_3)_4]^{2+}$, where the planar cation is positioned parallel to the dichalcogenide layer planes and requires only a relatively small expansion of the lattice; a starting two-phase region TaS$_2$/second stage was found with the limit at a charge transfer of $0.13\ e^-$/TaS$_2$ and an interlayer spacing $d = 15.3$ Å for the second-stage phase. The reaction of TaS$_2$ with the metallocene cation $(C_5H_5)_2Co^+$ is clearly a two-phase region TaS$_2$/first-stage phase up to $0.25\ e^-$/TaS$_2$, where a potential step

indicates the end of the reaction. The product $[(C_5H_5)_2Co^+]_{0.25}[TaS_2]^{0.25-}$ is identical in composition and lattice parameters ($a = 3.30$ Å, $c = 22.90$ Å) with samples prepared by thermal intercalation of the neutral metallocene in 2H–TaS$_2$ (13).

Kinetic reasons seem also to be involved in the intercalation of large organic cations by cathodic reduction. In Table II the interlayer spacing for a series of compounds with carbonium ions, aromatic ammonium ions, and cationic dye molecules obtained by cathodic reduction are listed. A defined two-phase starting region was found for anilinium ion $C_6H_5NH_3^+$ with the formation of a second-stage intermediate (range 0–$0.11\ e^-$/MX_2; $d = 18.6$ Å for second-stage product) and for p-phenylenediamine-H$^+$, for which a two-phase region second stage/first stage was observed (0–$0.13\ e^-$/

TABLE II

INTERLAYER SPACINGS d FOR INTERCALATION
COMPOUNDS OF 2H–TaS$_2$ WITH METAL
COMPLEX IONS AND ORGANIC CATIONS
OBTAINED BY CATHODIC REDUCTION

Cation	d (Å)
$[(C_5H_5)_2Co]^+$	11.45
$[(C_5H_6)_2Cr]^+$	11.91
$[Fe(dipyridine)_3]^{2+}$	14.92
$[Fe(phenanthroline)_3]^{2+}$	15.44
$[(NH_3)_3Co(OH)_3Co(NH_3)_3]^{3+}$	11.74
$[Cu(ethylenediamine)_2]^{2+}$	9.31
$[Pt(NH_3)_4]^{2+}$	9.18
$[Ba(crypt)]^{2+\ d}$	14.16
$(C_6H_5NH_3)^+$	12.83
$(H_2N–C_6H_4–NH_3)^+$	13.32
$[(CH_3)_2NH_2C_6H_4NH_2]^+$	12.21
$(acridine-H)^+$	12.34
$(C_{28}H_{31}N_2O_3)^{+\ a}$	16.8
$(C_{20}H_{20}N_3^+)^{\ b}$	12.52
$(C_7H_7)^{+\ c}$	13.15

[a] Rhodamine B.
[b] Fuchsine.
[c] Tropylium cation.
[d] crypt = 4, 7, 13, 16, 21, 24-hexaoxa-1, 10-diazabicyclo-(8, 8, 8)-hexacosane.

MX_2); the interlayer spacing of the first-stage phase corresponds to 9.29 Å, i.e., monolayers of aromatic rings with the ring plane positioned parallel to the dichalcogenide planes. Similar results were reported for the intercalation of pyridinium ions into 2H–TaS$_2$ by cathodic reduction (14). In the case of the larger aromatic molecules potential/charge transfer curves show strong deviations from equilibrium potential values at low current density; X-ray powder diagrams reveal the existence of broad diffraction lines at low 2Θ values at the beginning of cathodic reduction, although no pure phases could be isolated in this range.

The significant influence of the host lattice stacking modification on products and course of electrochemical reduction is demonstrated by a comparison of 2H–NbS$_2$ and 2H–TaS$_2$ (both trigonal prismatic coordination of intralayer cations) with the CdI$_2$-type phase 1T–TaS$_2$, where the intralayer transition metal cations reside in octahedral positions. While the reaction, e.g., with simple spherical hydrated cations is closely similar for both 2H forms and characterized by the regular occurrence of higher-stage intermediates and final products with a charge transfer of 0.5 e^-/MX_2, the reduction of 1T–TaS$_2$, e.g., in K$^+$/H$_2$O electrolyte results in a final reduction product K$^+_{0.3}$(H$_2$O)$_{0.7}$[TaS$_2$]$^{0.3-}$ with a lower negative layer charge density. A change in layer stacking sequence occurring on intercalation leads to a tripled c axis; hexagonal lattice constants found are $a = 3.39$ and $c = 27.664$ Å with $d = c/3 = 9.22$ Å. The reduction proceeds at constant potential and corresponds to a two-phase region 1T–TaS$_2$/K$_{0.3}$(H$_2$O)$_{0.7}$TaS$_2$; X-ray diffraction lines that can be attributed to higher-stage bulk nuclei are present in addition to first-stage product only directly after the start of the reaction but obviously turn over rapidly to first-stage product.

Several steps show up in potential/charge transfer curves for the cathodic reduction in aqueous alkali electrolytes of TiS$_2$ which also crystallizes in the CdI$_2$-type structure. At low reduction values diffraction lines of higher-stage products were detected. The 00l reflection series were found, however, to be nonintegral and could not yet be indexed unambiguously.

Conclusions

The formation of defined phase regions and of higher-stage products, respectively, were reported to occur in the course of chemical intercalation of unsolvated alkali metals (15) and on thermal intercalation of Lewis base molecules (16). No discrete intermediates were found for the intercalation of highly mobile unsolvated small cations, e.g., Cu$^+$ and Li$^+$. Recent studies on the systems Li$^+$/TiS$_2$ and Li$^+$/TaS$_2$ now present, however, evidence for the existence of domain-type ordering of Li$^+$ cations (8, 17). It is thus to be concluded that the presence of ordered intermediate states is a general phenomenon in the reaction mechanism of dichalcogenide intercalation.

The superiority in several aspects of neutron diffraction as compared to X-ray methods should particularly be of advantage in investigations under dynamic conditions of topotactic electrode reactions with highly mobile cations which are of potential technological importance in reversible battery systems. For a detailed understanding of these processes it is essential to correlate directly thermodynamic data and structural changes of the electrode in the course of charge and discharge cycles of real systems.

References

1. R. SCHÖLLHORN AND H. MEYER, *Mater. Res. Bull.* **9**, 1237 (1974).
2. M. S. WHITTINGHAM, *J. Chem. Soc. Chem. Commun.*, 328 (1974).
3. G. V. SUBBA RAO AND J. C. TSANG, *Mater. Res. Bull.* **9**, 921 (1974).

4. R. SCHÖLLHORN, E. SICK, AND A. LERF, *Mater. Res. Bull.* **10**, 1005 (1975).

5. A. LERF AND R. SCHÖLLHORN, *Inorg. Chem.* **16**, 2950 (1977).

6. C. RIEKEL AND R. SCHÖLLHORN, *Mater. Res. Bull.* **11**, 369 (1976).

7. C. RIEKEL, H. G. REZNIK, R. SCHÖLLHORN, AND C. J. WRIGHT, *J. Chem. Phys.* **70**, 5203 (1979).

8. R. R. CHIANELLI, J. C. SCANLON, AND B. M. L. RAO, *J. Electrochem. Soc.* **125**, 1563 (1978).

9. H. A. GRAF, A. LERF, AND R. SCHÖLLHORN, *J. Less Common Metals* **55**, 213 (1977).

10. U. RÖDER, W. MÜLLER-WARMUTH, AND R. SCHÖLLHORN, *J. Chem. Phys.* **70**, 2864 (1979).

11. C. RIEKEL AND C. O. FISCHER, *J. Solid State Chem.* **29**, 181 (1979).

12. N. DAUMAS AND A. HÉROLD, *C. R. Acad. Sci. Paris Ser. C* **268**, 373 (1969); G. SCHOPPEN, H. MEYER-SPASCHE, L. SIEMSGLÜSS, AND W. METZ, *Mater. Sci. Eng.* **31**, 115 (1977); J. M. THOMAS AND A. D. JEFFERSON, *Endeavour New Ser.* **2**, 127 (1978).

13. M. B. DINES, *Science* **188**, 1210 (1975); W. B. DAVIES, M. L. H. GREEN, AND A. J. JACOBSEN, *J. Chem. Soc. Chem. Commun.*, 781 (1976); R. P. CLEMENT, W. B. DAVIES, K. A. FORD, M. L. H. GREEN, AND A. J. JACOBSEN, *Inorg. Chem.* **17**, 2754 (1978).

14. R. SCHÖLLHORN, H. D. ZAGEFKA, T. BUTZ, AND A. LERF, *Mater. Res. Bull.* **14**, 369 (1979); R. SCHÖLLHORN, *Physica* **99B**, 89 (1980).

15. A. LeBLANC, M. DANOT, L. TRICHET, AND J. ROUXEL, *Mater. Res. Bull.* **9**, 191 (1974); J. ROUXEL, *J. Solid State Chem.* **17**, 223 (1976).

16. F. R. GAMBLE AND T. H. GEBALLE, *in* "Treatise on Solid State Chemistry" (N. B. Hannay, Ed.), Vol. 3, p. 89, Plenum, New York (1976).

17. T. BUTZ, H. SAITOVITCH, AND A. LERF, *Chem. Physics Lett.* **65**, 146 (1979); A. H. THOMPSON, *Phys. Rev. Lett.* **40**, 1511 (1978).